MNRAS 000, 1–12 (2015) Preprint 4 November 2015 Compiled using MNRAS LATEX style file v3.0

Comparing galaxy disk and star-formation properties in X-ray bright and faint groups and clusters

Ian D. Roberts,* Laura C. Parker, Ananthan Karunakaran
Department of Physics and Astronomy, McMaster University, Hamilton ON L8S 4M1, Canada

Accepted XXX. Received YYY; in original form ZZZ

arXiv:1511.01020v1 [astro-ph.GA] 3 Nov 2015

ABSTRACT

Galaxy morphologies and star-formation rates depend on environment. Galaxies in underdense regions are generally star-forming and disky whereas galaxies in overdense regions tend to be early-type and not actively forming stars. The mechanism(s) responsible for star-formation quenching and morphological transformation remain unclear, although many processes have been proposed. We study the dependence of star-formation and morphology on X-ray luminosity for galaxies in Sloan Digital Sky Survey Data Release 7 (SDSS-DR7) groups and clusters. While controlling for stellar and halo mass dependencies, we find that galaxies in X-ray strong groups and clusters have preferentially low star-forming and disk fractions – with the differences being strongest at low stellar masses. The trends that we observe do not change when considering only galaxies found within or outside of the X-ray radius of the host group. When considering central and satellite galaxies separately we find that this dependence on X-ray luminosity is only present for satellites, and we show that our results are consistent with "galaxy stangulation" as a mechanism for quenching these satellites. We investigate the dynamics of the groups and clusters in the sample, and find that the velocity distributions of galaxies beyond the virial radius in low X-ray luminosity halos tend to be less Gaussian in nature than the rest of the data set. This may be indicative of low X-ray luminosity groups and clusters having enhanced populations of star-forming and disk galaxies as a result of recent accretion.

Key words: galaxies: clusters: general – galaxies: evolution – galaxies: groups: – galaxies: statistics

1 INTRODUCTION

Numerous studies have shown a strong environmental dependence on the star-forming and morphological properties of galaxies (e.g. Butcher & Oemler 1978; Dressler 1980; Postman & Geller 1984; Dressler et al. 1999; Blanton et al. 2005b; Wetzel et al. 2012). Low density regimes tend to be dominated by star-forming, late-type galaxies whereas high density areas, such as galaxy clusters, tend to be primarily populated by quiescent, early-type galaxies. Within individual clusters, galaxy morphologies tend to distribute as a function of local density (or equivalently cluster-centric radius), with high fractions of late-type galaxies being found at large radii and the regions near the cluster core being dominated by early-types (e.g. Dressler 1980; Postman & Geller 1984; Postman et al. 2005). This effect has become known as the morphology-density relation. While galaxies tend to distribute based on their star-forming and morphological properties, the mechanism(s) responsible for the quenching of star-formation and morphological transformations in galaxies are not well constrained – although many have been proposed. Both mergers and impulsive galaxy-galaxy interactions ("harassment") (e.g. Moore et al. 1996) can induce star-burst events in galaxies leading to rapid consumption of gas reserves and star-formation quenching. Within the virial radius of a group or cluster the stripping of gas from galaxies becomes efficient. Both the stripping of hot halo gas ("strangulation") (e.g. Kawata & Mulchaey 2008) and cold gas stripping due to a dense intra-cluster medium ("ram-pressure") (e.g. Gunn & Gott 1972) can quench star-formation. As well, tidal interactions can affect gas reservoirs by transporting gas from the galactic halo outwards which subsequently allows it to more easily be stripped from the galaxy (Chung et al. 2007).

On top of these environmental quenching mechanisms, previous authors have found that secular processes, which depend on galaxy mass, appear to play a significant role in star-formation quenching (Balogh et al. 2004; Muzzin et al. 2012). The emergent picture for star -formation quenching appears to be some combination of environmental quenching mechanisms and internal, secular processes. In particular, Peng et al. (2010) suggests that in the low redshift Universe, environmental quenching is dominant for galaxies with $M_\star \lesssim 10^{10.5}\,\mathrm{M}_\odot$, whereas for galaxies with $M_\star \gtrsim 10^{10.5}\,\mathrm{M}_\odot$ mass quenching plays the more important role.

While environmental and mass quenching within individual

* E-mail: roberid@mcmaster.ca

© 2015 The Authors

halos are seemingly strong effects, it is important to realize that groups and clusters are not isolated structures. In particular, galaxies can be pre-quenched in group halos prior to infall into a larger cluster. This "pre-processing" suggests that many galaxies may already be quenched upon cluster infall. Simulations have shown that between ~ 25 and 45 per cent of infalling cluster galaxies may have been pre-processed (McGee et al. 2009; De Lucia et al. 2012). Observationally, Hou et al. (2014) find that ~ 25 per cent of the infall population reside in subhalos for massive clusters ($M_H \gtrsim 10^{14.5}\,\mathrm{M}_\odot$). This pre-quenching of galaxies in groups could potentially be driven by galaxy interactions and mergers which are favoured in the group regime as a result of lower relative velocities between member galaxies (Barnes 1985; Brough et al. 2006).

An important method for studying the quenching mechanisms in groups and clusters is to study the dependence of the star-formation and morphological properties of galaxies on the conditions of their host halo (e.g. halo mass, X-ray luminosity, etc.). In particular, if quenching mechanisms depend on the density of the intra-group/cluster medium (IGM/ICM) – for example, ram-pressure stipping of cold gas – then one would expect to see galaxy populations which are preferentially passive in halos with high X-ray luminosities. Such correlations have been looked for in previous studies, primarily within cluster environments.

In particular, Ellingson et al. (2001) finds no positive correlation between the fraction of old galaxies and X-ray gas density. Balogh et al. (2002a) conclude that the level of star-formation found in their "low-L_X" sample is consistent with the levels seen in their CNOC1 sample consisting of higher mass clusters. Fairley et al. (2002) and Wake et al. (2005) both study the fractions of blue galaxies at intermediate redshifts and find no discernible trend between blue fraction and X-ray luminosity. Using multivariate regression Popesso et al. (2007b) find that cluster star-formation depends on cluster richness but find no additional dependence on X-ray luminosity. In addition, they find no significant correlation between star-forming fraction and any global cluster property (M_{200}, σ_v, $N_{\rm gal}$, and L_X). Lopes et al. (2014) find no dependence of blue fraction on X-ray luminosity and the only slight dependence they find between disk fraction and X-ray luminosity is within the central and most dense regions.

Conversely, Balogh et al. (2002b) find that galaxies in their "low-L_X" sample have preferentially high disk fractions compared to galaxies in their "high-L_X" sample. Postman et al. (2005) find that the bulge-dominated fraction for galaxies in high X-ray luminosity clusters is higher than for those in low X-ray luminosity clusters. In contrast with their star-formation results, Popesso et al. (2007b) do find a significant anti-correlation between blue fraction and X-ray luminosity. Finally, Urquhart et al. (2010) find an anti-correlation between blue fraction and X-ray temperature for galaxies in intermediate redshift clusters.

In this paper we re-visit the dependence of galaxy star-formation and morphological properties on the X-ray luminosity of the host halo. Specifically, as a result of the large SDSS X-ray sample presented in Wang et al. (2014), we are able to control for stellar mass, halo mass, and radial dependencies through fine-binning of the data set. This allows us to more directly investigate the effect of X-ray luminosity on galaxies in different environments.

The results of this study are presented as follows. In § 2 we briefly describe the SDSS group catalogues utilized in this work, as well as the star-formation and morphology catalogues which we match to the group data set. In § 3 we present the primary results of this paper, specifically, the differences between star-forming and morphological trends in environments with different X-ray luminosities. In § 4 we provide a discussion of the results presented in this paper. Finally, in § 5 we provide a summary of the key results and make concluding statements.

In this paper we assume a Λ cold dark matter cosmology with $\Omega_M = 0.3$, $\Omega_\Lambda = 0.7$, and $H_0 = 70\,\mathrm{km\,s^{-1}\,Mpc^{-1}}$.

2 DATA

2.1 Yang group catalogue

This work relies heavily on the group catalog of Yang et al. (2007). The Yang group catalogue is constructed by applying the iterative halo-based group finder of Yang et al. (2005, 2007) to the New York University Value-Added Galaxy Catalogue (NYU-VAGC; Blanton et al. 2005a), which is based on the Sloan Digital Sky Survey Data Release 7 (SDSS-DR7; Abazajian et al. 2009). The Yang group catalogue has a wide range of halo masses, spanning from $\sim 10^{12}\,\mathrm{M}_\odot$ to $\sim 10^{15}\,\mathrm{M}_\odot$. The catalogue contains both objects which would be classified as groups ($10^{12} \lesssim M_H \lesssim 10^{14}\,\mathrm{M}_\odot$) and as clusters ($M_H \gtrsim 10^{14}\,\mathrm{M}_\odot$), however for brevity we will refer to all systems as groups regardless of mass.

Groups are initially populated using the traditional friends-of-friends (FOF) algorithm (e.g. Huchra & Geller 1982), as well as assigning galaxies not yet linked to FOF groups as the centres of potential groups. Next, the characteristic luminosity, $L_{19.5}$, defined as the combined luminosity of all group members with ${}^{0.1}M_r - 5\log h \leq -19.5$, is calculated for each group. Using the value of $L_{19.5}$ along with an assumption for the group mass-to-light ratio, $M_H/L_{19.5}$, a tentative halo mass is assigned on a group-by-group basis. The tentative halo mass is used to calculate a virial radius and velocity dispersion for each group, which are then used to add or remove galaxies from the system. Galaxies are assigned to groups under the assumption that the distribution of galaxies in phase space follows that of dark matter particles – the distribution of which is assumed to follow a spherical NFW profile (Navarro et al. 1997). This process is iterated until the group memberships no longer change.

Final halo masses given in the Yang group catalogue are determined using the ranking of the characteristic stellar mass, $M_{\star,\rm grp}$, and assuming a relationship between M_H and $M_{\star,\rm grp}$ (Yang et al. 2007). $M_{\star,\rm grp}$ is defined by Yang et al. as

$$M_{\star,\rm grp} = \frac{1}{g(L_{19.5}, L_{\rm lim})} \sum_i \frac{M_{\star,i}}{C_i}, \tag{1}$$

where $M_{\star,i}$ is the stellar mass of the ith member galaxy, C_i is the completeness of the survey at the position of that galaxy, and $g(L_{19.5}, L_{\rm lim})$ is a correction factor which accounts for galaxies missed due to the magnitude limit of the survey. The statistical error in M_H is on the order of 0.3 dex and mostly independent of halo mass (Yang et al. 2007).

2.2 SDSS X-ray catalogue

To study the X-ray properties of the group sample, we utilize the SDSS X-ray catalogue of Wang et al. (2014). Wang et al. use ROSAT All Sky Survey (RASS) X-ray images in conjuction with optical groups identified from SDSS-DR7 (Yang et al. 2007) to estimate X-ray luminosities around $\sim 65\,000$ spectroscopic groups..

To identify X-ray luminosities for individual groups, the algorithm of Shen et al. (2008) is employed. Beginning from an optical

group, the most massive galaxies (MMGs) of that group are identified – up to four MMGs are kept. The RASS fields in which the MMGs reside are then identified, and an X-ray source catalogue is generated in the 0.5 – 2.0 keV band. The maximum X-ray emission density point is used to identify the X-ray centre of the group, and any X-ray sources not associated with the group (e.g. point source quasars or stellar objects cross-matched from RASS and SDSS-DR7), within one virial radius, are masked out. Values for the X-ray background, centred on the X-ray centre, are determined and subtracted off and the X-ray luminosity, L_X, is calculated by integrating the source count profile within the X-ray radius.

Determining X-ray luminosities in this manner is susceptible to "source confusion". Due to projection it is possible for more than one group to contribute to the X-ray emission within the X-ray radius, leading to an overestimation of the X-ray luminosity for a given group. To account for this effect Wang et al. calculate the "expected" average X-ray flux, $F_{X,i}$, for each group using the average $L_X - M_H$ relation taken from Mantz et al. (2010). They then calculate the sum of the expected fluxes from each group for multi-group systems and determine the contribution fraction, $f_{\mathrm{mult},i}$, for each group defined as,

$$f_{\mathrm{mult},i} = F_{X,i}/\Sigma_i F_{X,i}. \quad (2)$$

The contribution factor will approximate the fraction of the observed X-ray luminosity intrinsic to the individual group in question, therefore applying this fraction to each group will act to debias the measured X-ray luminosity from source confusion contamination.

Within the Wang catalogue 817 groups have $S/N > 3$, compared to the total of 34522 groups with positive detections (positive count rates after background subtraction) and $S/N > 0$. We run our analysis for groups with $S/N > 3$ as well as groups with $S/N > 0$ and find that our choice of signal-to-noise cut does not change the trends that we observe, therefore we focus on the total sample ($S/N > 0$) to ensure a sample size which is large enough to finely bin the data in various properties simultaneously.

2.3 Final data set

To obtain the final data set, we match the Wang SDSS X-ray catalogue to the Yang SDSS group catalogue, giving us both optical and X-ray group properties for the sample. To obtain individual galaxy properties we further match the data set to various public SDSS catalogues, as follows.

We utilize stellar masses given in the NYU-VAGC, which are computed following the methodology of Blanton & Roweis (2007).

To obtain star-formation rates (SFRs) and specific star formation rates (SSFR = SFR/$M_\star$) we match the catalogue of Brinchmann et al. (2004) to the sample. SFRs given by Brinchmann et al. are determined using emission line fluxes whenever possible, however in the case of no clear emission lines or contamination from active galactic nuclei, SFRs are determined using the strength of the 4000 Å break (D_n4000) (Brinchmann et al. 2004).

We obtain galaxy morphologies from the catalogue of Simard et al. (2011). Simard et al. perform two-dimensional bulge + disk decompositions for over one million galaxies from the Legacy area of the SDSS-DR7, using three different fitting models: a pure Sérsic model, a bulge + disk model with de Vaucouleurs ($n_b = 4$) bulge, and a bulge + disk model with a free n_b. To distinguish between disky and elliptical galaxies we utilize the galaxy Sérsic index, n_g, from the pure Sérsic decomposition. We also use the V_{max} weights

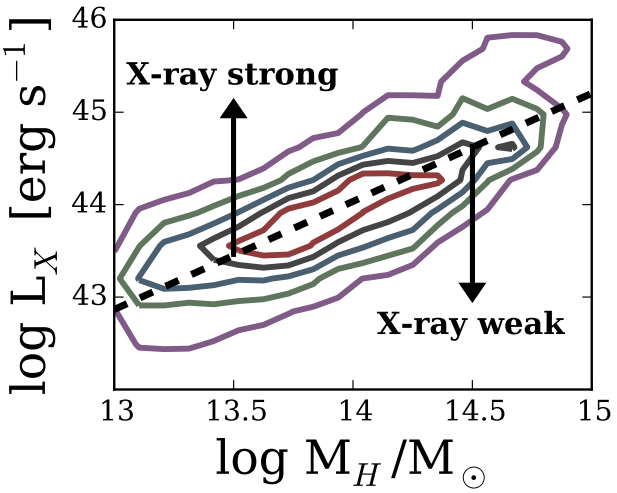

Figure 1. Density contours for log X-ray luminosity versus log halo mass. Dashed line corresponds to the linear least-squares best-fit relationship.

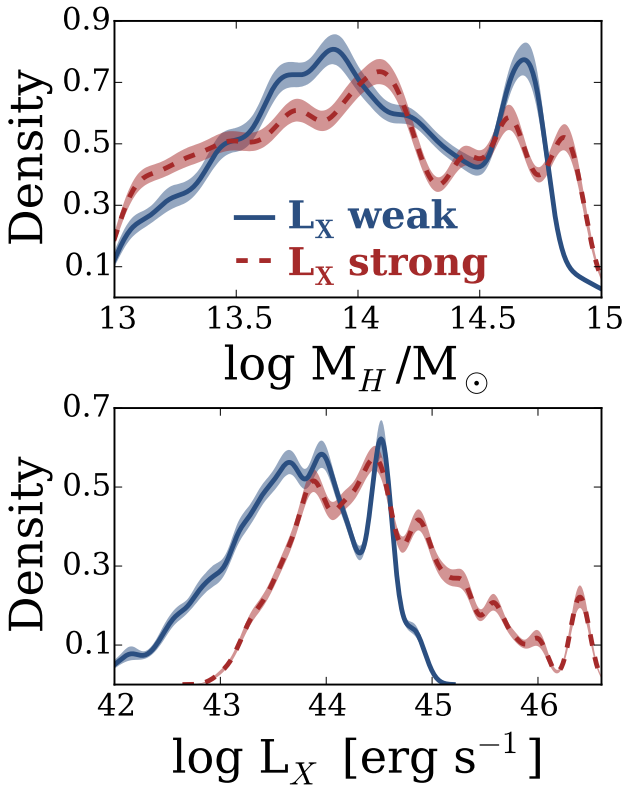

Figure 2. Smoothed distributions for halo mass and X-ray luminosity within the sample. Distributions are shown for both the X-ray strong (red, dashed) and the X-ray weak (blue, solid) samples. Shaded regions correspond to 2σ confidence intervals obtained from random bootstrap resampling.

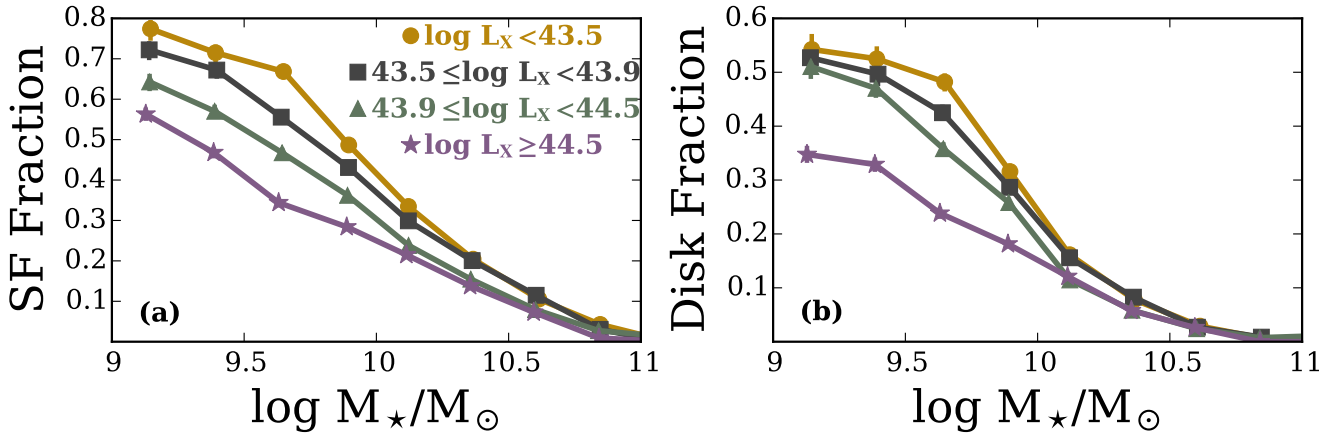

Figure 3. Left: star-forming fraction versus stellar mass for the four X-ray luminosity quartiles of the data sample. Right: disk fraction versus stellar mass for the four X-ray luminosity quartiles of the sample. Error bars correspond to 1σ Bayesian binomial confidence intervals given in Cameron (2011).

given by Simard et al. to correct for the incompleteness of our sample.

We calculate group-centric distances for each galaxy using the redshift of the group and the angular seperation between the galaxy and the luminosity-weighted centre of its host group. We normalize all of the galaxy radii by the virial radius of the host group, R_{180}, which we calculate as in Yang et al. (2007)

$$R_{180} = 1.26 h^{-1}\,\mathrm{Mpc}\left(\frac{M_H}{10^{14} h^{-1}\mathrm{M}_\odot}\right)^{1/3}(1+z_g)^{-1}, \quad (3)$$

where z_g is the redshift of the group center.

The final data set includes groups with halo masses ranging between $10^{13} - 10^{15}\,\mathrm{M}_\odot$, and galaxies with stellar masses ranging from $10^{9} - 10^{11.3}\,\mathrm{M}_\odot$. Group X-ray luminosities in the data set are between $10^{39.6} - 10^{46.4}\,\mathrm{erg\,s^{-1}}$, with a median value of $10^{43.9}\,\mathrm{erg\,s^{-1}}$, and are strongly correlated with halo mass (see Fig. 1). We do not make an explicit radial cut, however over 99 per cent of member galaxies fall within 1.5 virial radii. Our final sample contains 3902 low redshift ($z < 0.1$) groups housing a collective 41173 galaxies. The catalogue of Wang et al. (2014) contains $\sim$ 35000 groups, the fact that the final sample in this work is significantly smaller is for two reasons. Firstly, we restrict our sample to redshifts smaller than 0.1 which reduces the number of groups from $\sim$ 35000 at $z < 0.2$ to $\sim$ 18000 at $z < 0.1$. The second important cut is that we require $10^{13} < M_H < 10^{15}\,\mathrm{M}_\odot$, a number of groups in the Wang et al. catalogue have halo masses, $M_H < 10^{13}\,\mathrm{M}_\odot$ (where halo masses have been obtained from the catalogue of Yang et al. 2007), this cut reduces the remaining number of groups from $\sim$ 18000 to $\sim$ 3900. It should be noted that the majority of the $M_H < 10^{13}\,\mathrm{M}_\odot$ groups removed from the data set are groups with very low membership.

To determine the effect of X-ray luminosity on star-formation and morphology we consider two X-ray luminosity samples for the majority of our analysis, which we refer to as the X-ray weak (XRW) and X-ray strong (XRS) samples. Similar to Wang et al., we define the XRS sample to consist of all galaxies found above the best-fit $\log M_H - \log L_X$ line (see Fig. 1), and correspondingly the XRW sample consists of all galaxies found below the $\log M_H - \log L_X$ trend line. This leads to an approximately equal number of galaxies within the XRW and XRS samples. We also performed our analysis with a cut between the two X-ray samples at the median X-ray luminosity of the data set, as well as defining the two samples using the first and fourth quartiles, however these alternative definitions of the two X-ray samples do not change the trends that we observe.

Smoothed distributions for halo mass and X-ray luminosity are shown in Fig. 2 for both X-ray luminosity samples. Density distributions are calculated using the `density {stats}` function in the statistical computing language R (R Core Team 2013)[1] using a Gaussian kernel.

We study the dependence of star-formation rates and morphology on stellar mass by binning the data by stellar mass and calculating the disk and star-forming fractions for each bin. Binning by stellar mass is important to account for the systematic dependence of star-formation and morphology on stellar mass (e.g. Brinchmann et al. 2004; Whitaker et al. 2012). Additionally, as the relative balance between environmental and mass quenching is not well understood, it is important to investigate the effects of environment at a given stellar mass.

We define the star-forming fraction, f_{SF}, as the fraction of galaxies in each bin with $\log \mathrm{SSFR} > -11$. Wetzel et al. (2012) show that at low redshift the division between the red sequence and the blue cloud is found at $\log \mathrm{SSFR} \simeq -11$ across a wide range of halo masses. For each stellar mass bin the star-forming fraction is given by

$$f_{SF} = \frac{V_{\max}\text{ weighted \# galaxies with } \log SSFR > -11}{V_{\max}\text{ weighted total \# galaxies}}. \quad (4)$$

Similarly we define the disk fraction, f_D, as the fraction of galaxies in each bin with Sérsic index, $n < 1.5$. For each stellar mass bin this is given by

$$f_D = \frac{V_{\max}\text{ weighted \# galaxies with } n < -1.5}{V_{\max}\text{ weighted total \# galaxies}}. \quad (5)$$

We also ran our analysis using a dividing cut at Sérsic indices of $n = 1.0$ and $n = 2.0$ to define a disk galaxy, however using these

[1] http://www.R-project.org/

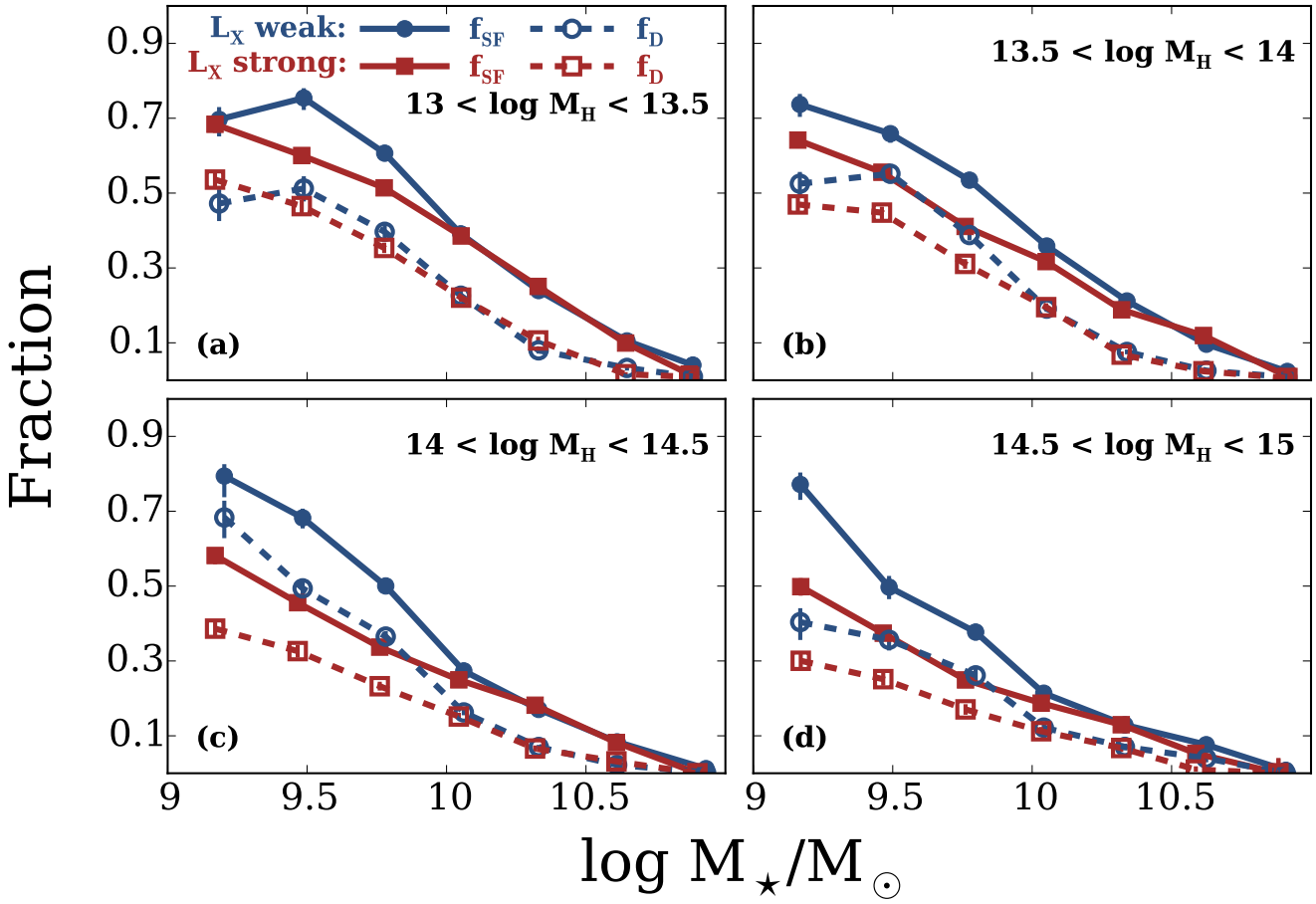

Figure 4. Star-forming (solid lines) and disk (dashed lines) fractions versus stellar mass, for different halo mass bins and the XRW (blue) and XRS (red) samples. Error bars correspond to 1σ Bayesian binomial confidence intervals given in Cameron (2011).

alternative definitions for a disk galaxy does not alter the trends that we observe.

3 RESULTS

3.1 Star-forming and morphology trends in strong and weak L_X samples

To investigate the effect of X-ray luminosity on galaxy properties, in Fig. 3 we show star-forming and disk fractions, as a function of stellar mass, for subsamples corresponding to the four X-ray luminosity quartiles of the data set. Examination of Fig. 3a and 3b show that star-forming and disk fractions follow a consistent marching order with respect to X-ray luminosity. The disk and star-forming fractions decrease as X-ray luminosity increases.

We note that the results in Fig. 3 consider all halo masses in the sample, however it has been found that galaxy morphology and star-formation depend on local density and halo mass (Dressler 1980; Balogh et al. 2004; Wetzel et al. 2012; Lackner & Gunn 2013) (however also see: De Lucia et al. 2012; Hoyle et al. 2012; Hou et al. 2013). As shown in Fig. 1 the data show a strong correlation between X-ray luminosity and halo mass, therefore we must determine if differences shown in Fig. 3 are simply a result of galaxies in higher L_X environments being housed in preferentially high-mass halos.

To control for any potential halo mass effect, we further bin the data into narrow halo mass bins and re-examine the dependence of galaxy properties on X-ray luminosity, considering now the XRW and XRS samples from Fig. 1. Fig. 4 shows star-forming (solid) and disk (dashed) fractions as a function of stellar mass for four different halo mass bins – ranging from $10^{13} - 10^{15}\,M_\odot$ with bin widths of 0.5 dex. Data are binned according to stellar mass and markers are plotted at the median bin values. For each halo mass bin we show star-forming and disk fractions from the X-ray strong and X-ray weak samples.

For both star-forming and disk fractions we continue to see a residual trend with X-ray luminosity, even after controlling for any halo mass dependence: star-forming and disk fractions are systematically higher in the XRW sample. We see the strongest trends in the intermediate and high mass halos. The difference between the strong (red) and the weak (blue) X-ray luminosity samples is clearest at low stellar mass, and in all halos the two samples converge at moderate to high stellar mass.

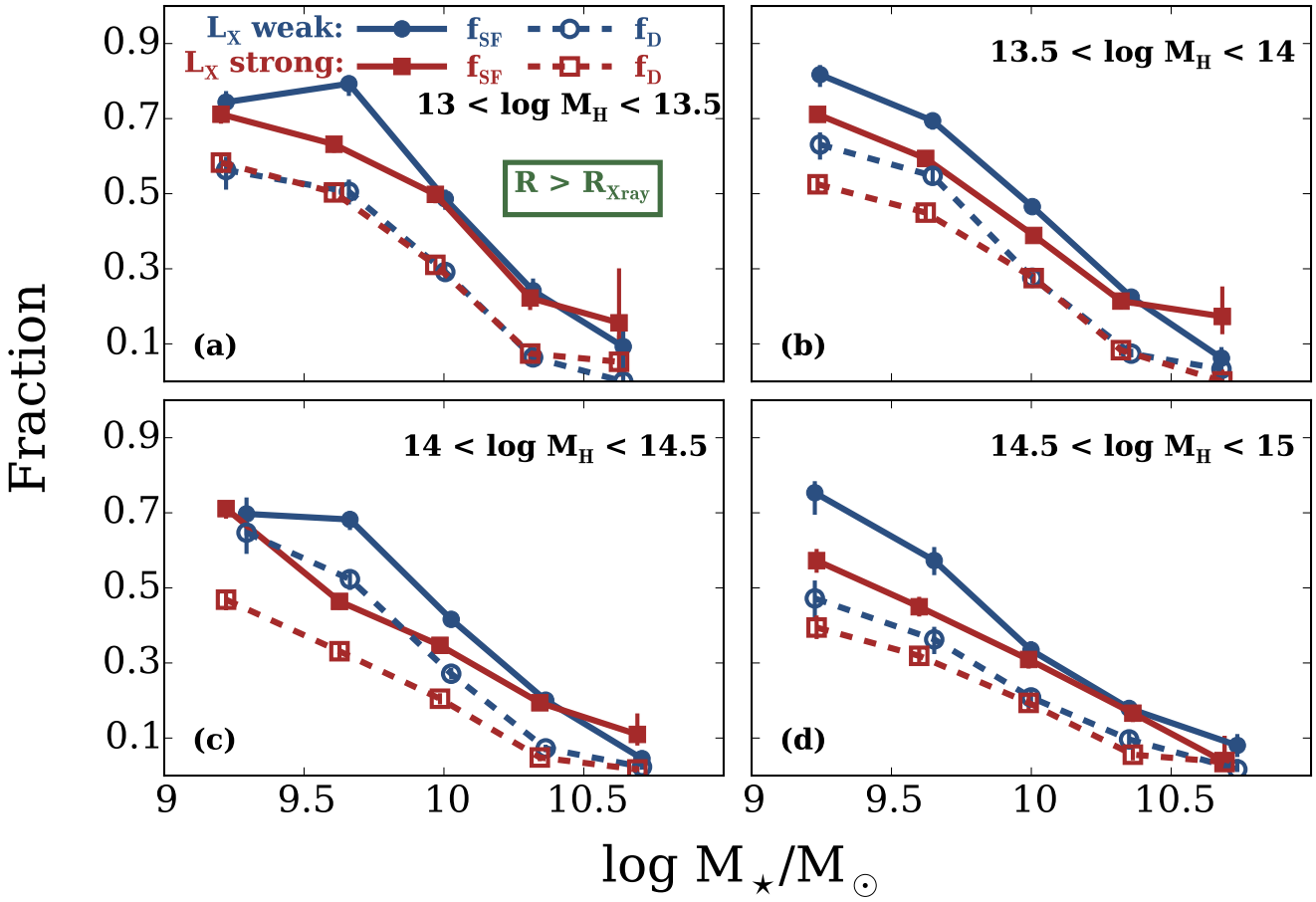

Figure 5. Star-forming (solid lines) and disk (dashed lines) fractions versus stellar mass, for galaxies outside of their host X-ray radius and for different halo mass bins and the two L_X samples. Error bars correspond to 1σ Bayesian binomial confidence intervals given in Cameron (2011).

3.2 Radial dependence of star-forming and morphology trends

Within host groups X-ray emission is concentrated at relatively small group-centric radii, with X-ray emission generally extending out to half a virial radius (Wang et al. 2014). If the trends we are observing are a result of increased gas density, we would expect to see enhanced trends (i.e. a larger difference between the XRS and XRW samples) at small group-centric radii and suppressed trends at large radii. To test this we further divide the data into subsets corresponding to those galaxies that lie within the X-ray emission radius (using the X-ray radius, R_{Xray}, given in Wang et al. 2014) and those galaxies that lie outside of the X-ray radius. We again plot star-forming/disk fraction versus stellar mass, in narrow halo mass bins, for the large and small radius subsamples. The results of this analysis are shown in Fig. 5 & 6, where the two figures correspond to disk fraction and star-forming fraction trends for the large and small radius subsamples, respectively.

Examination of Fig. 5 & 6 shows that for both galaxies found within their host halo's X-ray radius, and those found outside, we still see an increase in star-forming and disk fractions in the XRW sample – as before this effect is strongest in the intermediate to high mass halos and at low stellar mass. Also the disk and star-forming fractions tend to be higher at large radii, which is consistent with the morphology-density relation.

To further investigate if the increase in star-forming and disk fractions in the XRW sample compared to the XRS sample – which we will refer to as the "SF excess" and the "disk excess" – depends on whether you consider galaxies within or outside the X-ray radius, we show SF and disk excess versus stellar mass in Fig. 7. We quantitatively define SF and disk excess as

$$\text{SF excess} = f_{SF}(XRW) - f_{SF}(XRS) \quad (6)$$

$$\text{Disk excess} = f_{D}(XRW) - f_{D}(XRS), \quad (7)$$

where $f_{SF}(XRW)$ and $f_{SF}(XRS)$ are the star-forming fractions in the XRW and XRS samples respectively, and analogously for $f_D(XRW)$ and $f_D(XRS)$.

We find no radial dependence for SF and disk excess as the two radial subsamples in Fig. 7 show overlap for all halo and stellar masses. With the exception in Fig 7c where the SF excess, for low-mass galaxies, is stronger for galaxies within the X-ray radius.

4 DISCUSSION

We find that star-forming and disk fractions are systematically lower in the XRS sample than galaxies in XRW environments. This trend persists even upon controlling for any halo mass dependence, however the observed difference between the XRS and the

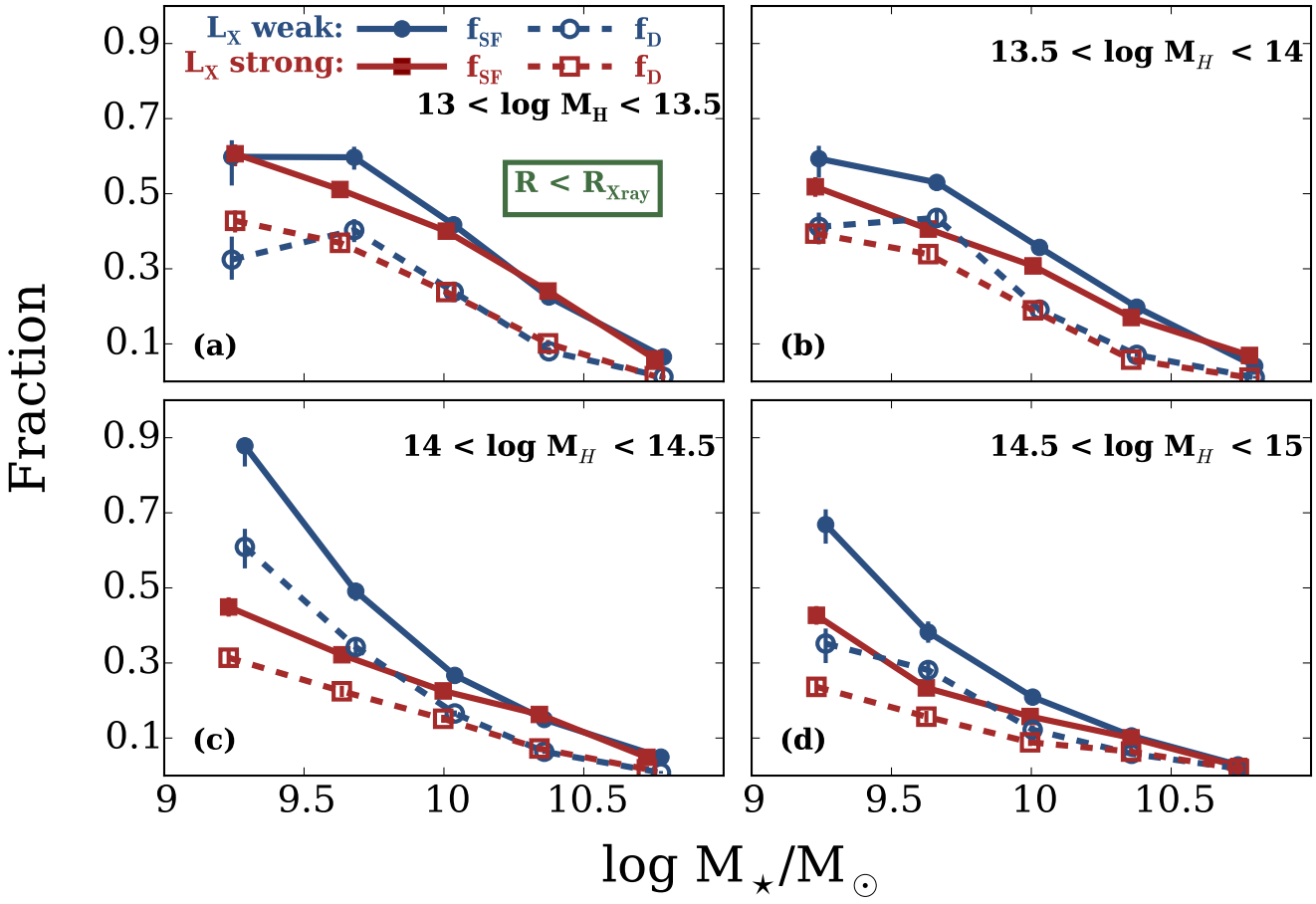

Figure 6. Same as Fig. 5 for galaxies inside of their host X-ray radius.

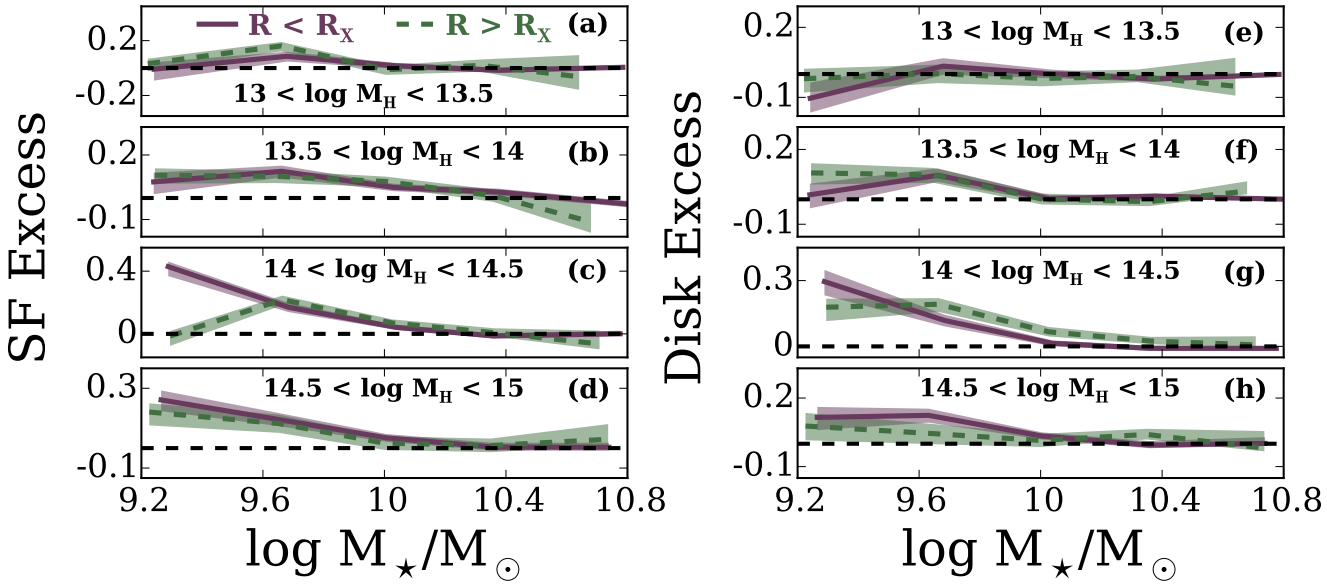
R < R_X
R > R_X
13 < log M_H < 13.5 (a)
13.5 < log M_H < 14 (b)
14 < log M_H < 14.5 (c)
14.5 < log M_H < 15 (d)
13 < log M_H < 13.5 (e)
13.5 < log M_H < 14 (f)
14 < log M_H < 14.5 (g)
14.5 < log M_H < 15 (h)
SF Excess
Disk Excess
log M_⋆/M_⊙

Figure 7. SF and disk excess versus stellar mass for both galaxies within (purple, solid) and outside (green, dashed) of the X-ray radius. Panels a-d show SF excess for four halo mass bins and panels e-h show disk excess for four halo mass bins. Shaded regions represent 1σ confidence intervals.

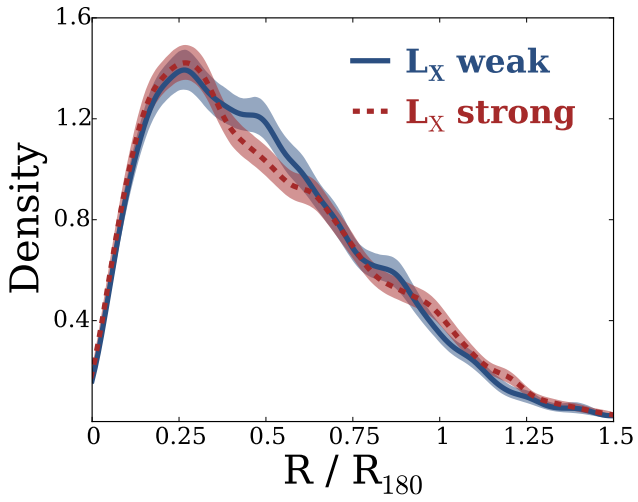

Figure 8. Smoothed radial distributions of galaxies in the XRW (blue, solid) and XRS (red, dashed) samples. Shaded regions correspond to 2σ confidence intervals obtained from random bootstrap resampling.

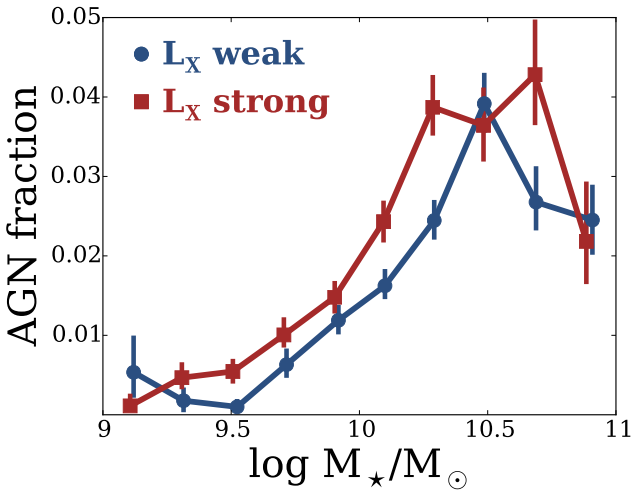

Figure 9. BPT identified AGN fraction versus stellar mass for our XRW and XRS samples. Error bars correspond to 1σ Bayesian binomial confidence intervals given in Cameron (2011).

XRW sample is not enhanced when considering only those galaxies within the X-ray radius of the host halo.

There are two major observed effects which have been found to impact the distributions of early-type and late-type galaxies within cluster environments. The so called "Butcher-Oemler" (BO) effect is the observational trend that the blue fraction of cluster galaxies are positively correlated with redshift (e.g. Butcher & Oemler 1984; Ellingson et al. 2001; Loh et al. 2008; Urquhart et al. 2010). However, it should be noted that there is still debate when it comes to the physical nature of the BO effect (for example, see: Andreon & Ettori 1999; Andreon et al. 2004, 2006). Since we are only considering low-redshift ($z < 0.1$) galaxies the BO effect should be negligible.

The second major effect is the previously mentioned morphology-density relationship. In order to determine if the morphology-density relation is affecting the trends we observe, we must check if there are significant differences in the radial distributions of the XRS and the XRW samples. For instance, if the XRW sample is found at systematically high group-centric radii compared to the XRS sample, then the morphology-density relation could explain why we find systematically larger star-forming and disk fractions in the XRW sample. In Fig. 8 we plot the smoothed radial distributions for both the XRS and the XRW samples. We see no systematic difference between the two distributions, in fact they are nearly indistinguishable from one another. We conclude that the two X-ray samples have radial distributions which do not differ substantially from one another, and therefore any observed differences between the XRS and XRW samples are not being driven by differing radial distributions.

4.1 AGN contamination

When considering X-ray properties of galaxy groups it is important to ensure that the observed X-ray emission is due to the hot IGM and not due to contamination from AGN or other X-ray sources. In Wang et al. (2014) bright point sources, such as stars and quasars, are masked out, however it is still important to ensure that our results are not being contaminated by galaxies housing non point source AGN.

In Fig. 9 we plot AGN fraction versus stellar mass for the XRW and XRS samples. We use AGN classified by Kauffmann et al. (2003), which are identified using the location of galaxies on the BPT diagram (Baldwin et al. 1981). It should be noted that Trouille & Barger (2010) show that between 20 and 50 per cent (depending on the dividing line between AGN and star-formings galaxies used) of X-ray identified AGN fail to be classified as AGN on the BPT diagram.

We see that the AGN fraction tends to be larger within the XRS sample, however at all stellar masses the number of AGN galaxies is a modest fraction (less than five per cent) of the total sample, for both XRS and XRW galaxies. Most relevant is the fact that at low stellar mass the AGN fraction is consistently below one per cent, for both the XRW and XRS samples, and that the trends that we observe with X-ray luminosity are exclusively seen at low stellar mass (e.g. Fig 4). We examined disk and star-forming fractions for a subsample of the data with galaxies identified as AGN removed and found that removing AGN galaxies from the sample does not change the observed trends. Furthermore, we examined trends after removing all groups that house galaxies identified as AGN and again found no change in the observed trends. Therefore we conclude that AGN are not a significant contributor to the observed trends in star-forming and disk fractions.

4.2 Implications for star-formation quenching

The relative importance of various galaxy quenching mechanisms is an important, open question. Galaxy populations in groups can be classified as either "central" (located at the centre of the group dark matter halo) or "satellite" galaxies. These two populations are expected to evolve differently (e.g. van den Bosch et al. 2008), and therefore when attempting to elucidate information on the quenching of galaxies it is important to consider centrals and satellites as distinct populations. In Fig. 10 we plot SF and disk excess (Equations 6 & 7) versus stellar mass, considering separately central and satellite galaxies. Central galaxies are defined as the most massive

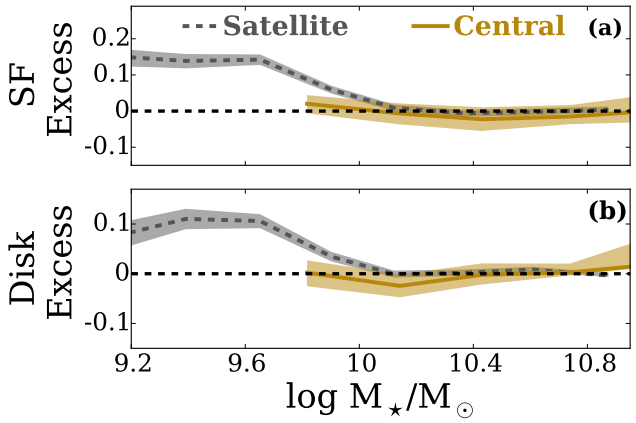

Figure 10. SF and disk excess versus stellar mass for both centrals (gold, solid) and satellites (gray, dashed). Shaded regions correspond to 1σ confidence intervals.

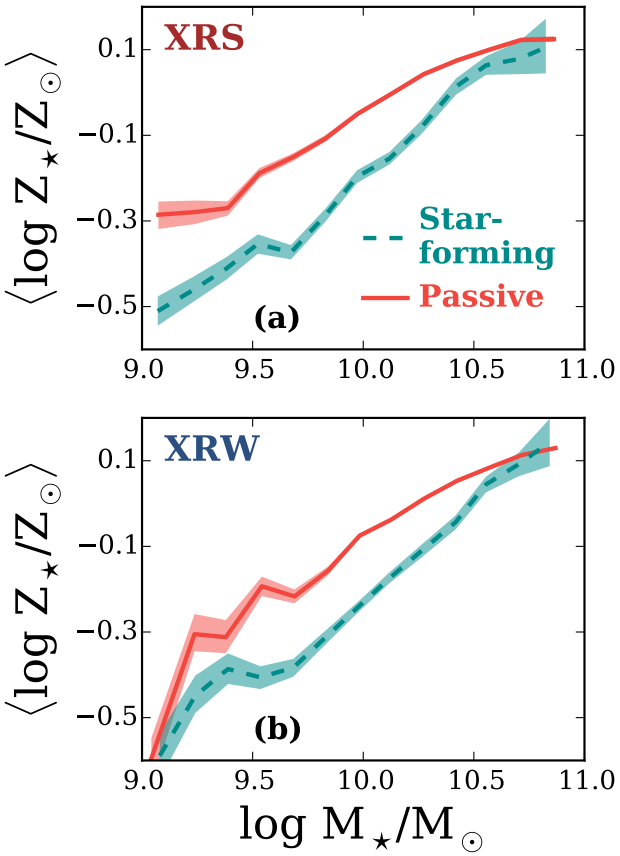

Figure 11. Mean stellar metallicity versus stellar mass for star-forming (blue, dashed) and passive (red, solid) galaxies, divided by galaxies in the XRS (top) and XRW (bottom) samples. Shaded regions correspond to 1σ confidence intervals obtained from random bootstrap resampling.

group galaxies and satellite galaxies are defined as all group galaxies which have not been classified as centrals.

When considering satellite galaxies in Fig. 10a we find that galaxies within the XRW sample have consistently larger star-forming fractions at low stellar mass (SF excess > 0), while at large stellar mass the XRW and XRS samples are indistinguishable. When considering only central galaxies we find that there is no difference between the XRW and XRS samples (SF excess ≈ 0) when considering star-forming fraction. We observe qualitatively similar trends for disk excess in Fig. 10b. This implies that whatever effect X-ray luminosity has on star-forming and morphlogical properties it only affects satellite galaxies, central galaxies are insensitive to the group X-ray properties. This is not surprising given that central galaxies are massive, and we see no difference between the XRS and XRW at large stellar mass.

One interpretation of the differences we observe between the XRW and XRS samples would be to invoke the ram-pressure stripping of satellite galaxies. The rate at which galaxies will lose gas through ram-pressure stripping will increase in proportion to L_X (Fairley et al. 2002). Therefore, if ram-pressure is an important mechanism when it comes to the quenching of galaxies, a decrease in star-forming fraction should be observed with increasing X-ray luminosity. It be noted that although we observe very similar trends for star-forming and disk fractions, it is not clear whether ram-pressure stripping can efficiently drive galaxy morphology transformations from late to early type (Christlein & Zabludoff 2004). Prior studies (e.g. Gavazzi et al. 2003; Kenney et al. 2004; Muzzin et al. 2014) have found evidence of ram-pressure stripping. We note as well that other studies (e.g. Balogh et al. 2002a; Fairley et al. 2002; Wake et al. 2005; Lopes et al. 2014) have found no clear trend between star-forming or blue fractions and X-ray luminosity. At first glance the results shown in Fig. 4 are consistent with ram pressure stripping; at low stellar masses there are lower star-forming fractions in the XRS sample. One difference between the results we observe and previous studies is that we narrowly bin our data in stellar mass. Since star-forming and morphological properties depend strongly on stellar mass, any residual dependence on X-ray luminosity may be lost without controlling for stellar mass. In addition our sample size is significantly larger than most previous studies, so it may be that trends with X-ray luminosity are subtle enough to be missed without large statistics.

If the trends we detect are driven by ram-pressure we would expect a radial dependence of our trends with X-ray luminosity. The efficiency of ram-pressure stripping is proportional to ρv^2 (Wake et al. 2005; Popesso et al. 2007b), where ρ is the IGM density and v is the speed of the member galaxies. Since the IGM density is highest at small group-centric radii, the efficiency of ram-pressure stripping should increase towards small radii. In Fig. 7 we showed that the observed SF excess does not strongly depend on radius. We conclude that this lack of radial dependence is inconsistent with the ram-pressure stripping scenario.

Another often envoked mechanism for regulating star-formation is "galaxy strangulation" (Larson et al. 1980; Balogh et al. 2000; Kawata & Mulchaey 2008; Peng et al. 2015). Strangulation is a mechanism in which the replenishment of cold gas onto galaxies is halted, which in turn leads to galaxy quenching once the galaxy has exhausted its existing cold gas reservoirs. The timescales over which a galaxy will be quenched by strangulation are longer than the quenching times associated with the direct stripping of cold gas reserves (ram-pressure). Recently, Peng et al. (2015) have argued that it is possible to differentiate between strangulation and direct stripping using metallicity differences between star-forming and quiescent galaxy populations. We direct the reader to Peng et al. (2015) for a more complete discussion, however the main idea is that quenching by strangulation will result in higher metallicities for passive galaxies compared to star-forming

galaxies. This is a result of star-formation continuing even after the gas supply has been halted which will increase stellar metallicity until the cold gas reserves have been exhausted and the galaxy has therefore been quenched. This trend in metallicity is not expected from direct stripping, where star-formation shuts off quickly after the removal of cold gas.

To investigate the effect of strangulation on the galaxy sample in this study we follow Peng et al. and calculate mean stellar metallicity versus stellar mass considering star-forming and passive galaxies separately, for galaxies within our XRW sample as well as our XRS sample. Metallicities are matched to our sample from the catalogue of Gallazzi et al. (2005), and mean metallicities are plotted in stellar mass bins with widths of 0.15 dex. Not all of the galaxies within this sample have measured metallicities, therefore for this aspect of the analysis our XRW and XRS samples are reduced to 10939 (52 per cent of total sample) and 8851 (44 per cent of total sample) member galaxies, respectively.

In Fig. 11 we see higher stellar metallicities for passive galaxies compared to star-formers, which we interpret as evidence for strangulation playing a significant role in star-formation quenching. Of particular interest for this work is the behaviour at low stellar mass which is where the dependence of star-formation and morphology on X-ray luminosity is observed (see Fig. 4). We see a somewhat stronger strangulation signal (ie. difference between passive and star-former metallicity) for galaxies in the XRS sample compared to the XRW sample, at low stellar mass.

In light of this observed difference, it important to note that compiling this subsample of galaxies with measured metallicities does not affect all stellar masses equally. Specifically, low-mass galaxies are preferentially removed from the sample when matching to the metallicity catalogue. In particular, 69 per cent of low-mass ($M_\star < 10^{9.5}\,\mathrm{M}_\odot$) galaxies in the XRS sample do not have measured metallicities, whereas in the XRW sample 75 per cent of low-mass galaxies do not have measured metallicities. Not only are low-mass galaxies being preferentially lost, but the fraction of low-mass galaxies being lost is slightly different between the two X-ray samples. Therefore, although the results in Fig. 11 are consistent with strangulation – and more specifically, somewhat stronger strangulation at the low-mass end of the XRS sample – we suggest that this trend be interpretted with caution as completeness differences could be playing some role.

4.3 Group evolutionary/dynamical state

The dynamical state of galaxy groups is an important evolutionary indicator and can potentially have an impact on galaxy properties. Trends with X-ray luminosity may reflect that the XRW and XRS samples have different dynamical properties as it is expected that more evolved groups with relaxed dynamics would be more X-ray luminous (Popesso et al. 2007a).

Theoretically the velocity distribution of galaxies within a group in dynamical equilibrium should have a characteristic Gaussian shape. Groups lacking this Gaussian distribution can therefore be considered as being unevolved, dynamically young systems. To investigate the dependence on the dynamical state of the groups in our data set we follow the procedure of Hou et al. (2009) and apply the Anderson-Darling normality (ADN) test to the velocity distributions of the galaxies in the group sample. The ADN test is a non-parametric test which compares the cumulative distribution function (CDF) of the data to the CDF of a normal distribution to determine the probability (p-value) that the difference between the distribution of the data and that of a Gaussian is as large as observed (or larger), under the assumption that the data is in fact normally distributed. For our dynamical analysis we use a subset of the data consisting of only those groups with eight or more members (31820 galaxies in 1456 groups), in order to ensure reasonable statistics when applying the ADN test. To obtain values for the ADN statistic for each of our groups we employ the `ad.test {nortest}` function in the statistical computing language `R` (R Core Team 2013) – large values of the ADN statistic are indicative of less Gaussian distributions.

Initially, we examine the dynamical states of galaxies within the XRW and XRS samples globally (i.e. no radial cuts) and we find no systematic differences between the dynamical states of XRW and XRS galaxies. Popesso et al. (2007a) study the difference between X-ray underluminous Abell (AXU) clusters and normal Abell clusters. They find that while both AXU and normal Abell clusters show Gaussian velocity distributions within the virialized region ($R < 1.5\,R_{200}$), within the exterior regions ($1.5\,R_{200} \leq R \leq 3.5\,R_{200}$) the AXU clusters show sharply peaked, non-Gaussian velocity distributions. The authors interpret these leptokurtic velocity distributions in the outer cluster regions as evidence that AXU clusters have experienced recent accretion/merging. If the XRW groups have experienced more recent accretion of galaxies from the field and smaller groups than the XRS groups, then this could contribute to the dependence we observe between star-forming and disk fractions on X-ray luminosity. Galaxies in underdense regions (the field, low-mass groups) have been found to be preferentially star-forming with late-type morphologies. Accordingly, groups experiencing recent accretion may contain more star-forming, late-type, galaxies when compared to groups which are dynamically older.

To investigate this possibility we study the dynamical states of groups in both the XRW and XRS samples, and divide member galaxies into two radial subsamples: those found in the inner regions ($R < R_{180}$) of their host group, and those found in the outer regions ($R \geq R_{180}$) of their host group. This is similar to the analysis performed by Popesso et al. (2007a). Instead of making an arbitrary, discrete cut to define Gaussian and non-Gaussian groups we treat the AD statistic values as continuous and compare the distributions of ADN statistics from the four subsamples (XRW inner, XRW outer, XRS inner, XRS outer) to determine whether there are any significant differences in dynamical states. To quantitatively compare the distributions we utilize the two-sample Anderson Darling (AD2) test. The AD2 test is similar to the ADN test, however instead of comparing observed data to the normal distribution, it compares the CDFs of two data samples to determine whether they are drawn from the same underlying distribution. We apply the AD2 test to the distributions of ADN statistic values for the XRW and XRS samples to determine if the dynamical states vary between the inner and outer regions. To perform the AD2 test between the subsamples we use the `ad.test {kSamples}` function in the statistical computing language `R` (R Core Team 2013).

We find no evidence (p-value = 0.38) for different dynamical states in the inner and outer regions of the XRS sample, however for the XRW sample we find strong evidence (p-value = 3×10^{-7}) that the dynamical state of galaxies in the outer region is different from those in the inner region. When we examine the distributions of ADN statistics for the four subsamples we find that the ADN statistic values for the XRW outer subsample are systematically higher than for the other three subsamples. This suggests that the velocity distributions for galaxies outside of the virial radius in the XRW sample are less Gaussian than the rest of the data set.

This result is consistent with Popesso et al. (2007a), who find

non-Gaussian velocity distributions for galaxies in the outer regions of X-ray underluminous Abell clusters. This result supports the notion that the increased number of star-forming and late-type galaxies we observe in the XRW sample can potentially be explained by underluminous X-ray groups experiencing recent accretion of field galaxies and small galaxy groups, as this recent accretion can give rise to less Gaussian velocity distributions in the exteriors of these groups.

We do note that it remains difficult to simultaneously explain the dynamical results together with the fact that we observe no dependence of SF and disk excess on radius (Fig. 7).

5 SUMMARY & CONCLUSIONS

We have used a sample of galaxies taken from X-ray emitting groups and clusters in the SDSS to study the effect of X-ray luminosity on galaxy star-formation and morphological properties. Using a data set spanning a large range in stellar mass ($10^9 - 10^{11.3}\,M_\odot$), halo mass ($10^{13} - 10^{15}\,M_\odot$), and X-ray luminosity ($10^{39.6} - 10^{46.4}\,erg\,s^{-1}$) we have investigated the differences between disk and star-forming fractions within different X-ray environments. The main results of this paper are as follows:

(i) Star-forming and disk fractions are preferentially lower within the X-ray strong sample when compared to galaxies within the X-ray weak sample – this trend remains after controlling for any halo mass dependence.

(ii) This difference between the X-ray strong and X-ray weak samples is most apparent at intermediate to high halo mass and at low stellar mass.

(iii) The differences we observe between the X-ray weak and X-ray strong samples do not depend on whether we consider galaxies inside of, or outside their host halo's X-ray radius.

(iv) The enhancement of star-forming and disk fractions we observe in the X-ray weak sample is present for satellites but not central galaxies, which is not surprising given that the difference between X-ray samples is only seen at low stellar mass.

(v) Our results are consistent with quenching by strangulation, in particular we see a somewhat stronger strangulation signal at low stellar mass within the XRS sample.

(vi) We find that in the X-ray weak sample the velocity distributions of galaxies outside of the virial radius are less Gaussian than galaxies within the virial radius. We find no differences between the dynamical states of inner and outer galaxies within the X-ray strong sample.

With the large sample of SDSS X-ray and spectroscopic groups we are able to study star-forming and disk fractions while simultaneously controlling for stellar mass, halo mass, and radial depedencies, thereby allowing a robust analysis of the effects of X-ray luminosity on star formation and morphology.

We find that galaxies outside the virial radius of X-ray underluminous groups have dynamics which are less Gaussian than the other groups in the sample. This may indicate that recent accretion onto low X-ray luminosity groups contributes to an excess of star-forming, late-type galaxies. The fact that the X-ray weak sample shows weaker stangulation could simply be due to the lower L_X environment reducing the efficiency of strangulation, or it could be a result of recently accreted galaxies having had less time to be quenched by environmental quenching mechanisms like stangulation. Naively, one would expect to observe a corresponding enhancement of star-forming, late-type galaxies in the exteriors of low X-ray luminosity groups compared to X-ray strong groups; however this is not observed. The results presented in this work therefore require a detailed theoretical treatment to fully explain the trends observed.

ACKNOWLEDGMENTS

We thank the anonymous referee for their various helpful comments and suggestions which have improved the paper. IDR and LCP thank the National Science and Engineering Research Council of Canada for funding. The authors thank F. Evans for matching together the various SDSS catalogues used in this research. We thank X. Yang et al. for making their SDSS DR7 group catalogue publicly available, L. Simard et al. for the publication of their SDSS DR7 morphology catalogue, J. Brinchmann et al. for publication of their SDSS SFRs, G. Kauffmann et al. for the publication of SDSS AGN galaxies, the NYU-VAGC team for the publication of their SDSS DR7 catalogue, and A. Gallazzi et al. for making publicly available their SDSS metallicities. This research would not have been possible without access to these public catalogues.

Funding for the SDSS has been provided by the Alfred P. Sloan Foundation, the Participating Institutions, the National Science Foundation, the U.S. Department of Energy, the National Aeronautics and Space Administration, the Japanese Monbukagakusho, the Max Planck Society, and the Higher Education Funding Council for England. The SDSS Web Site is http://www.sdss.org/.

The SDSS is managed by the Astrophysical Research Consortium for the Participating Institutions. The Participating Institutions are the American Museum of Natural History, Astrophysical Institute Potsdam, University of Basel, University of Cambridge, Case Western Reserve University, University of Chicago, Drexel University, Fermilab, the Institute for Advanced Study, the Japan Participation Group, Johns Hopkins University, the Joint Institute for Nuclear Astrophysics, the Kavli Institute for Particle Astrophysics and Cosmology, the Korean Scientist Group, the Chinese Academy of Sciences (LAMOST), Los Alamos National Laboratory, the Max-Planck-Institute for Astronomy (MPIA), the Max-Planck-Institute for Astrophysics (MPA), New Mexico State University, Ohio State University, University of Pittsburgh, University of Portsmouth, Princeton University, the United States Naval Observatory, and the University of Washington.

REFERENCES

Abazajian K. N., et al., 2009, ApJS, 182, 543
Andreon S., Ettori S., 1999, ApJ, 516, 647
Andreon S., Lobo C., Iovino A., 2004, MNRAS, 349, 889
Andreon S., Quintana H., Tajer M., Galaz G., Surdej J., 2006, MNRAS, 365, 915
Baldwin J. A., Phillips M. M., Terlevich R., 1981, PASP, 93, 5
Balogh M. L., Navarro J. F., Morris S. L., 2000, ApJ, 540, 113
Balogh M., Bower R. G., Smail I., Ziegler B. L., Davies R. L., Gaztelu A., Fritz A., 2002a, MNRAS, 337, 256
Balogh M. L., et al., 2002b, ApJ, 566, 123
Balogh M. L., Baldry I. K., Nichol R., Miller C., Bower R., Glazebrook K., 2004, ApJ, 615, L101
Barnes J., 1985, MNRAS, 215, 517
Blanton M. R., Roweis S., 2007, AJ, 133, 734
Blanton M. R., et al., 2005a, AJ, 129, 2562
Blanton M. R., Eisenstein D., Hogg D. W., Schlegel D. J., Brinkmann J., 2005b, ApJ, 629, 143

Brinchmann J., Charlot S., White S. D. M., Tremonti C., Kauffmann G., Heckman T., Brinkmann J., 2004, MNRAS, 351, 1151
Brough S., Forbes D. A., Kilborn V. A., Couch W., 2006, MNRAS, 370, 1223
Butcher H., Oemler Jr. A., 1978, ApJ, 219, 18
Butcher H., Oemler Jr. A., 1984, ApJ, 285, 426
Cameron E., 2011, PASA, 28, 128
Christlein D., Zabludoff A. I., 2004, ApJ, 616, 192
Chung A., van Gorkom J. H., Kenney J. D. P., Vollmer B., 2007, ApJ, 659, L115
De Lucia G., Fontanot F., Wilman D., 2012, MNRAS, 419, 1324
Dressler A., 1980, ApJ, 236, 351
Dressler A., Smail I., Poggianti B. M., Butcher H., Couch W. J., Ellis R. S., Oemler Jr. A., 1999, ApJS, 122, 51
Ellingson E., Lin H., Yee H. K. C., Carlberg R. G., 2001, ApJ, 547, 609
Fairley B. W., Jones L. R., Wake D. A., Collins C. A., Burke D. J., Nichol R. C., Romer A. K., 2002, MNRAS, 330, 755
Gallazzi A., Charlot S., Brinchmann J., White S. D. M., Tremonti C. A., 2005, MNRAS, 362, 41
Gavazzi G., Cortese L., Boselli A., Iglesias-Paramo J., Vílchez J. M., Carrasco L., 2003, ApJ, 597, 210
Gunn J. E., Gott III J. R., 1972, ApJ, 176, 1
Hou A., Parker L. C., Harris W. E., Wilman D. J., 2009, ApJ, 702, 1199
Hou A., et al., 2013, MNRAS, 435, 1715
Hou A., Parker L. C., Harris W. E., 2014, MNRAS, 442, 406
Hoyle B., Masters K. L., Nichol R. C., Jimenez R., Bamford S. P., 2012, MNRAS, 423, 3478
Huchra J. P., Geller M. J., 1982, ApJ, 257, 423
Kauffmann G., et al., 2003, MNRAS, 346, 1055
Kawata D., Mulchaey J. S., 2008, ApJ, 672, L103
Kenney J. D. P., van Gorkom J. H., Vollmer B., 2004, AJ, 127, 3361
Lackner C. N., Gunn J. E., 2013, MNRAS, 428, 2141
Larson R. B., Tinsley B. M., Caldwell C. N., 1980, ApJ, 237, 692
Loh Y.-S., Ellingson E., Yee H. K. C., Gilbank D. G., Gladders M. D., Barrientos L. F., 2008, ApJ, 680, 214
Lopes P. A. A., Ribeiro A. L. B., Rembold S. B., 2014, MNRAS, 437, 2430
Mantz A., Allen S. W., Ebeling H., Rapetti D., Drlica-Wagner A., 2010, MNRAS, 406, 1773
McGee S. L., Balogh M. L., Bower R. G., Font A. S., McCarthy I. G., 2009, MNRAS, 400
Moore B., Katz N., Lake G., Dressler A., Oemler A., 1996, Nature, 379, 613
Muzzin A., et al., 2012, ApJ, 746, 188
Muzzin A., et al., 2014, ApJ, 796, 65
Navarro J. F., Frenk C. S., White S. D. M., 1997, ApJ, 490, 493
Peng Y.-j., et al., 2010, ApJ, 721, 193
Peng Y., Maiolino R., Cochrane R., 2015, Nature, 521, 192
Popesso P., Biviano A., Böhringer H., Romaniello M., 2007a, A&A, 461, 397
Popesso P., Biviano A., Romaniello M., Böhringer H., 2007b, A&A, 461, 411
Postman M., Geller M. J., 1984, ApJ, 281, 95
Postman M., et al., 2005, ApJ, 623, 721
R Core Team 2013, R: A Language and Environment for Statistical Computing. R Foundation for Statistical Computing, Vienna, Austria
Shen S., Kauffmann G., von der Linden A., White S. D. M., Best P. N., 2008, MNRAS, 389, 1074
Simard L., Mendel J. T., Patton D. R., Ellison S. L., McConnachie A. W., 2011, ApJS, 196, 11
Trouille L., Barger A. J., 2010, ApJ, 722, 212
Urquhart S. A., Willis J. P., Hoekstra H., Pierre M., 2010, MNRAS, 406, 368
Wake D. A., Collins C. A., Nichol R. C., Jones L. R., Burke D. J., 2005, ApJ, 627, 186
Wang L., et al., 2014, MNRAS, 439, 611
Wetzel A. R., Tinker J. L., Conroy C., 2012, MNRAS, 424, 232
Whitaker K. E., van Dokkum P. G., Brammer G., Franx M., 2012, ApJ, 754, L29
Yang X., Mo H. J., van den Bosch F. C., Jing Y. P., 2005, MNRAS, 356, 1293
Yang X., Mo H. J., van den Bosch F. C., Pasquali A., Li C., Barden M., 2007, ApJ, 671, 153
van den Bosch F. C., Aquino D., Yang X., Mo H. J., Pasquali A., McIntosh D. H., Weinmann S. M., Kang X., 2008, MNRAS, 387, 79

This paper has been typeset from a TEX/LATEX file prepared by the author.